Journal of Sound and Vibration (1998) **212**(4), 663–683

AN EFFICIENT ALGORITHM FOR DYNAMIC ANALYSIS OF BRIDGES UNDER MOVING VEHICLES USING A COUPLED MODAL AND PHYSICAL COMPONENTS APPROACH

K. Henchi

GIREF and Department of Civil Engineering, Laval University, Quebec, Canada G1K 7P4

M. Fafard

GIREF and Department of Civil Engineering, Laval University, Quebec, Canada G1K 7P4

M. Talbot

Ministry of Transportation, Bridge Division, Quebec, Canada G1S 4X9

AND

G. Dhatt

Department of Mechanical Engineering, INSA de Rouen, 76130 Mont-Saint-Aignan, France

(*Received* 20 *June* 1997, *and in final form* 5 *December* 1997)

A general and efficient method is proposed for the resolution of the dynamic interaction problem between a bridge, discretized by a three-dimensional finite element model, and a dynamic system of vehicles running at a prescribed speed. The resolution is easily performed with a step-by-step solution technique using the central difference scheme to solve the coupled equation system. This leads to a modified mass matrix called a pseudo-static matrix, for which its inverse is known at each time step without any numerical effort. The method uses a modal superposition technique for the bridge components. The coupled system vectors contain both physical and modal components. The physical components are the degrees of freedom of a vehicle modelled as linear discrete mass–spring–damper systems. The modal components are the degrees of freedom of a linear finite element model of the bridge. In this context, the resolution of the eigenvalue problem for the bridge is indispensable. The elimination of the interaction forces between the two systems (bridge and vehicles) gives a unique coupled system (supersystem) containing the modal and physical components. In this study, we duly consider the bridge pavement as a random irregularity surface. The comparison between this study and the uncoupled iterative method is performed.

1. INTRODUCTION

Bridge response induced by moving vehicles is an important aspect in design and structural evaluation of bridges. Generally, bridge engineers use the dynamic amplification factor defined as the maximum of dynamic response on the maximum static response to a design or evaluation of bridge capacity. However, behind this factor, there are a lot of phenomena that influence the bridge behaviour (response). Many experimental studies [1–4] have shown that the impact factor is function of different parameters. These important

0022–460X/98/190663 + 21 $25.00/0/sv971459

parameters are: the characteristics of the vehicles (natural frequencies), the velocity of the vehicles, the characteristics of the bridge (natural frequencies), the road roughness profile of the bridge surface, and multiple vehicles and their transverse positions.

It is obvious that a simple beam model cannot precisely represent two- or three-dimensional behaviour, particularly in the case of a moving vehicle with paths that are not along the centreline of the bridge. For those reasons, the bridges will be modelled here with shell, plate and beam elements, while the vehicles will be modelled with two- or three-dimensional models [5–11].

The moving vehicle loads are time-dependent, because the position of wheel loads change with time and the suspension of vehicle oscillates, due to irregularities of the bridge deck and bridge vertical displacement under tires.

There are two ways to simulate the dynamic interaction between bridge and vehicles (Figure 1). The first one is based on the uncoupled iteration method [1, 5–8, 10, 11], in which each system (bridge and vehicles) is solved separately and an iterative process in each time step is performed to find the equilibrium between the bridge and vehicle tires. For the vehicles with linear suspension types, see references [5–8, 10–12].

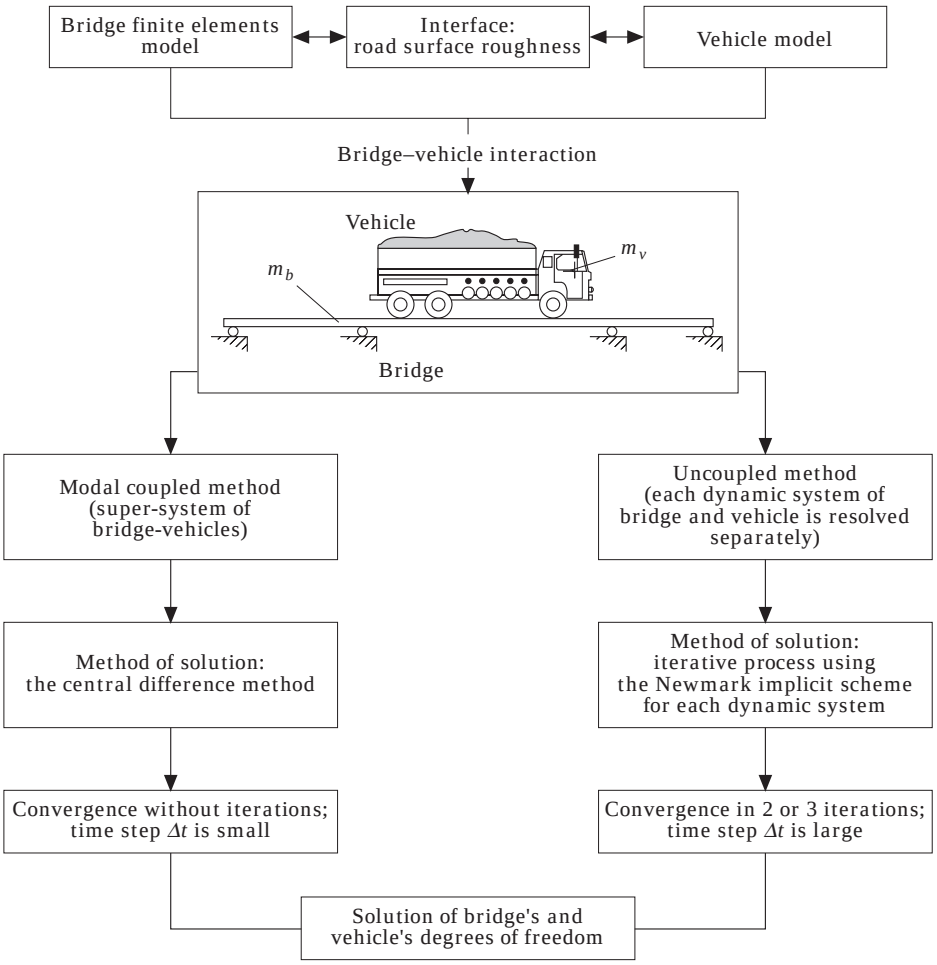

Figure 1. Dynamic analysis procedures for bridge and vehicles interaction.

The other way to simulate the dynamic interaction between bridge and vehicle consists of solving the super system fully coupled, and the solution is given at each time step without any iteration.

In this paper, we present an explicit algorithm technique to solve the coupled dynamic system using a modal superposition method for the bridge structure and the physical components for the vehicles using Lagrange's formulation. Thus, the coupled system vectors contain both modal and physical components. The former are the degrees of freedom in the modal space of the bridge and the latter are the degrees of freedom of the vehicles modelled as a linear discrete mass–spring–damper system. The model takes account of the road roughness through the power spectral density function [1, 13, 14], the constant speed of each vehicle, the multiple vehicles at different positions under different trajectories and the dynamic linear behaviour of vehicles and the bridge.

This method presents advantages and disadvantages. Among some advantages, we can quote the following: the CPU time is reduced in comparison with the uncoupled iterative method; easy and compact numerical implementation (super-system of bridge-vehicles); reduced computer memory storage; no factorization of the global matrix; no iteration in the computational process.

However, the principal disadvantages are as follows: modal projection in subspace is indispensable, and if the high frequencies of the bridge participate to the response this will create a problem in the dynamic response; this method is well adapted only for a few number of vehicles present on the bridge at the same time (this remark also applies to the uncoupled modal iterative method).

2. PROBLEM FORMULATION

2.1. ROAD SURFACE ROUGHNESS

The randomness of the bridge surface roughness can be described by a periodically modulated random process. It is specified by its power spectral density function (PSD) [1, 13, 14], which is given by

$$S_r(\omega_s) = A_r(\omega_s/\omega_{s0})^{-2}, \tag{1}$$

where $S_r(\omega_S)$ is the power spectral density (PSD) in m^2/cycle/m, A_r is the roughness coefficient in m^2/cycle/m, ω_{s0} is the discontinuity frequency equal to $1/2\pi$ (cycle/m) and ω_S is the spatial frequency in cycle/m.

From the PSD, a surface profile is generated using the FFT algorithm [13, 14] with the Monte Carlo simulation, to generate a random number φ distributed uniformly between 0 and 2π. The road profile in its discrete form is given by [8]

$$\mathbf{r}(x) = \sum_{k=1}^{N} \left(4A_r \left(\frac{2\pi k}{L_c \omega_{s0}} \right)^{-2} \frac{2\pi}{L_c} \right)^{1/2} \cos(\omega_{sk} x - \varphi_k), \tag{2}$$

where $\Delta\omega_s = 2\pi/L_c$, $\omega_{sk} = k\Delta\omega_s$, and L_c is, in general, twice the length of the bridge.

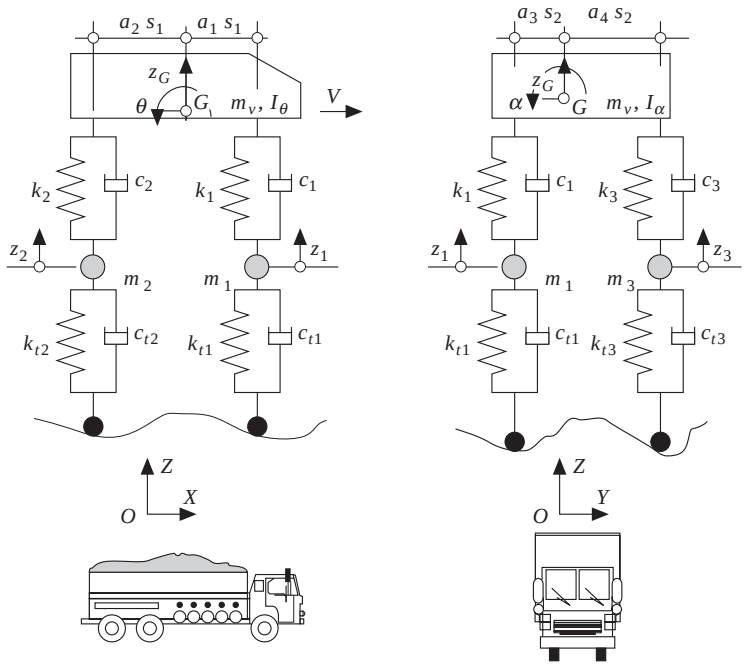

Figure 2. A 3-D vehicle with seven degrees of freedom (dof).

2.2. VEHICLE MODEL

The vehicle model is presented in Figure 2 [5–8, 15]. The equations of motion of the system are derived using Lagrange's formulation [3] as

$$\frac{\mathrm{d}}{\mathrm{d}t}\left(\frac{\partial T}{\partial \dot{q}_i}\right) - \frac{\partial T}{\partial q_i} + \frac{\partial V}{\partial q_i} - \frac{\partial W_d}{\partial \dot{q}_i} = Q_i \tag{3}$$

for each of the respective generalized co-ordinates. In equation (3), T and V are, respectively, the kinematic and potential energy of the system, q_i and ith generalized co-ordinate, W_d is the dissipation energy of the system and Q_i is the corresponding generalized force. When we apply equation (3) to each vehicle model, the equations of motion of the vehicle are

$$[\mathbf{M}_v]\{\ddot{\mathbf{Z}}\} + [\mathbf{C}_v]\{\dot{\mathbf{Z}}\} + [\mathbf{K}_v]\{\mathbf{Z}\} = \{\mathbf{F}_g\} - \{\overline{\mathbf{F}}^{int}\}, \tag{4}$$

where $\{\overline{\mathbf{F}}^{int}\}$ is the interaction force vector applied on the vehicle, $\mathbf{F}_g$ is the force vector caused by the effect of the gravitation; $[\mathbf{M}_v]$, $[\mathbf{C}_v]$ and $[\mathbf{K}_v]$ are, respectively, the mass, damping and stiffness matrices of the vehicle and $\{\mathbf{Z}\}$ is the vertical displacement vector of the vehicle degrees of freedom.

2.3. BRIDGE MODEL

The equations of motion for a bridge discretized by finite elements [5–8, 15] are

$$[\mathbf{M}_b]\{\ddot{\mathbf{U}}\} + [\mathbf{C}_b]\{\dot{\mathbf{U}}\} + [\mathbf{K}_b]\{\mathbf{U}\} = \{\mathbf{F}_{bv}^{int}\}. \tag{5}$$

The projection of equation (5) in the modal space of dimension **r** gives the following modal equations, if we use the classical Rayleigh damping matrix:

$$[\mathbf{I}]\{\ddot{\mathbf{y}}\} + [\boldsymbol{\chi}]\{\dot{\mathbf{y}}\} + [\boldsymbol{\Omega}]\{\mathbf{y}\} = [\boldsymbol{\Phi}]^{\mathrm{T}}\{\mathbf{F}_{bv}^{int}\}, \tag{6}$$

$$[\mathbf{I}] = \begin{bmatrix} \ddots & & \\ & 1 & \\ & & \ddots \end{bmatrix}_{r \times r}, \qquad [\boldsymbol{\chi}] = \begin{bmatrix} \ddots & & \\ & 2\xi_j\omega_j & \\ & & \ddots \end{bmatrix}_{r \times r}, \qquad [\boldsymbol{\Omega}] = \begin{bmatrix} \ddots & & \\ & \omega_j^2 & \\ & & \ddots \end{bmatrix}_{r \times r},$$

$$\{\mathbf{U}\} = \sum_{j=1}^{r} \{\phi_j\}\, y_j = [\boldsymbol{\Phi}]\{\mathbf{y}\}, \qquad \text{or at element level, } \{u^e\} = [\boldsymbol{\Phi}^e]\{y\}. \tag{7}$$

Matrix $[\boldsymbol{\Phi}]$ contains r mode shape vectors. In general, six degrees of freedom are assigned to each node (three translations and three rotations).

2.4. BRIDGE–VEHICLE INTERACTION

The interaction force of the ith wheel between the bridge and the vehicle is given by

$$\overline{F}_i^{int} = -F_{bv}^{int} i = k_{ti}\Delta_i + c_{ti}\dot{\Delta}_i. \tag{8}$$

k_{ti} and c_{ti} are, respectively, the tire stiffness and tire damping of the ith wheel (Figures 3 and 4), and Δ_i is the relative vertical displacement between the ith wheel and the bridge deck: $\Delta_i = -z_i + r_i + \bar{w}_i$, where z_i is the vertical displacement of the ith wheel, r_i is the road surface roughness under the ith wheel and $\bar{w}_i$ is the bridge vertical displacement under the ith wheel.

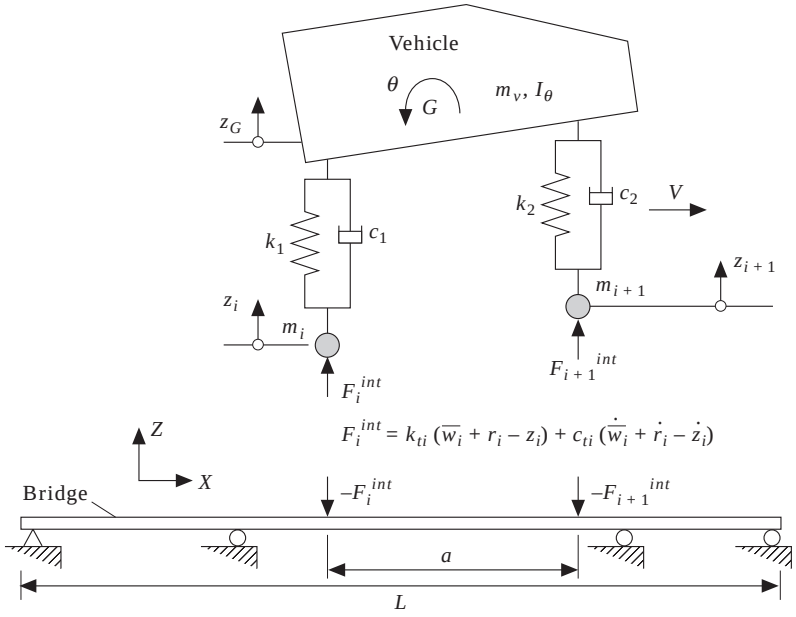

Figure 3. Bridge/vehicle interaction at wheel i.

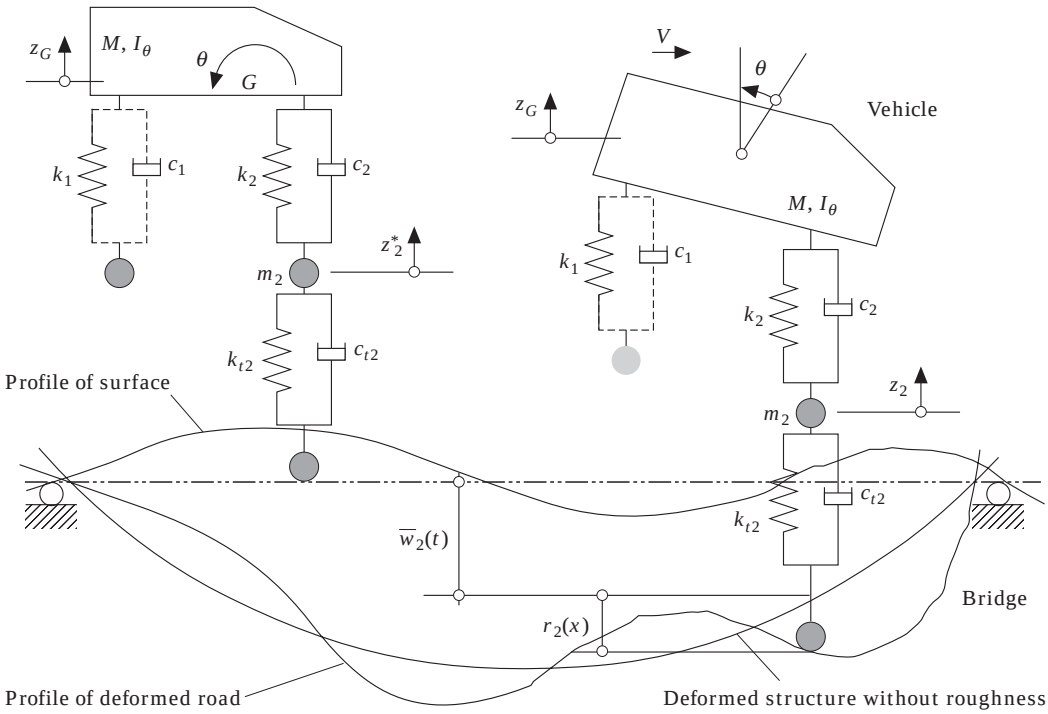

Figure 4. Bridge/vehicle interaction and bridge pavement effects, for a simple 2-D vehicle.

In a finite element context, $\bar{w}$ can be obtained using the following equation, where N_j are the shape functions and w_j^e the nodal displacements of the neighbourhood nodes of the ith wheel–bridge point of contact:

$$\bar{w} = \sum_{j=1}^{NN} N_j w_j^e = \langle \tilde{N} \rangle_i \{\mathrm{U}\}.$$

Note that $\{\tilde{N}\}_i$ and $\{N\}_j$ are equivalent with only different dimensions (Figure 5).

3. COMPUTATIONAL ALGORITHM

We now present the original algorithm based on a pseudo-static modified mass matrix. We first take the equations of motion (6), where the interaction nodal force vector applied by the vehicles on the bridge is

$$\{\mathbf{F}_{bv}^{int}\} = \sum_{i=1}^{nt} \{\tilde{N}\}_i F_{bvi}^{int}, \tag{9}$$

where $\{\tilde{N}\}_i$ is the vector of the shape functions evaluated at the location of the ith wheel and nt is the number of wheels. F_{bvi}^{int} is given here by

$$F_{bvi}^{int} = k_{ti}(z_i - (\bar{w}_i + r_i)) + c_{ti}(\dot{z}_i - (\dot{\bar{w}}_i + \dot{r}_i)), \tag{10}$$

with

$$\bar{w} + r(x) = \langle \tilde{N} \rangle \{\mathbf{U}\} + r(x), \tag{11}$$

$$\dot{\bar{w}} + \dot{r}(x) = \bar{w}_{,x}\dot{x} + \bar{w}_{,t} + \dot{r}(x) = \langle \tilde{N}_{,x} \rangle \{\mathbf{U}\}\dot{x} + \langle \tilde{N} \rangle \{\mathbf{U}_{,t}\} + r_{,x}\dot{x}. \tag{12}$$

Vectors $\{\mathbf{U}\}$ and $\{\mathbf{U}_{,t}\}$ are, respectively, the nodal displacements and velocities. If we replace $\bar{w}$, $\dot{\bar{w}}$, $r(x)$ and $\dot{r}(x)$ in equation (10) and use equation (7), with $v = \dot{x}$, we obtain

$$F_{bvi}^{int} = k_{ti}(z_i - (\langle \tilde{N} \rangle_i [\mathbf{\Phi}]\{y\} + r_i)) + c_{ti}(\dot{z}_i - ((v\langle \tilde{N}_{,x} \rangle_i [\mathbf{\Phi}]\{y\} + \langle \tilde{N} \rangle_i [\mathbf{\Phi}]\{\dot{y}\}) + \dot{r}_i)). \tag{13}$$

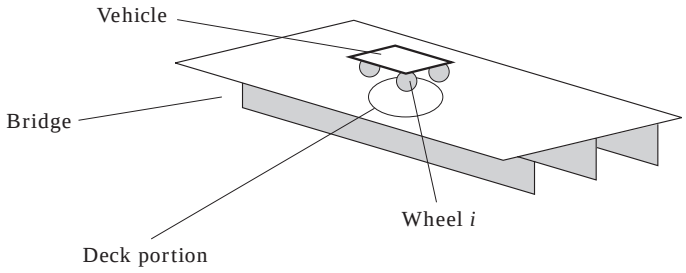

(a)

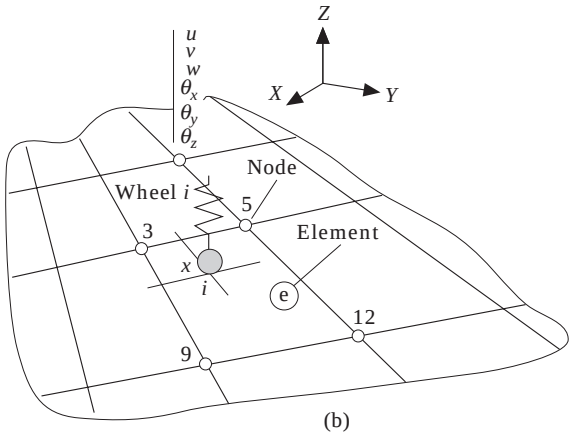

(b)

Nodes

3 5 9 12

$$\langle N \rangle_i = \langle N_1(x), (N_2(x), N_3(x), N_4(x) \rangle \quad \text{(in vertical direction)}$$

$$\langle \tilde{N} \rangle_i = \langle \underbrace{0,0,0,\ldots,0,0,}_{\text{Node 3}} \underbrace{N_1(x),0,0,0,0,0,0,\ldots,0,0,}_{\text{Node 5}} \underbrace{N_2(x),0,0,0,0,0,0,\ldots}_{\text{Node 5}}$$
$$\ldots,0,0, \underbrace{N_3(x),0,0,0,0,0,0,\ldots,0,0,}_{\text{Node 9}} \underbrace{N_4(x),0,0,0,0,0,\ldots,0}_{\text{Node 12}} \rangle$$

Figure 5. An example to illustrate the equivalence between the two vectors $\langle N \rangle_i$ and $\langle \tilde{N} \rangle_i$ under the ith wheel: (a) global bridge model; (b) finite element model of bridge deck portion.

With this last equation, equation (6) becomes a system of r coupled equations:

$$[\mathbf{I}]\{\ddot{\mathbf{y}}\} + \left([\boldsymbol{\chi}] + [\boldsymbol{\Phi}]^{\mathrm{T}}\left(\sum_{i=1}^{nt} \{\tilde{N}\rangle_i c_{ti} \langle \tilde{N}\rangle_i\right)[\boldsymbol{\Phi}]\right)\{\dot{y}\}$$

$$+ \left([\boldsymbol{\Omega}] + [\boldsymbol{\Phi}]^{\mathrm{T}}\left(\sum_{i=1}^{nt} \{\tilde{N}\}_i k_{ti} \langle \tilde{N}\rangle_i + \{\tilde{N}\}_i c_{ti} v \langle \tilde{N}_{,x}\rangle_i\right)[\boldsymbol{\Phi}]\right)\{y\}$$

$$= [\boldsymbol{\Phi}]^{\mathrm{T}} \sum_{i=1}^{nt} \{\tilde{N}\}_i (k_{ti}(z_i - r_i) + c_{ti}(\dot{z}_i - \dot{r}_i)). \tag{14}$$

The equations of motion of the vehicles are given by equation (4), where the interaction force applied by the bridge on the ith wheel of the vehicle is

$$\bar{F}_i^{int} = k_{ti}(\bar{w}_i + r_i) + c_{ti}(\dot{\bar{w}}_i + \dot{r}_i) \tag{15}$$

and the vector of forces applied to all wheels is

$$\{\bar{\mathbf{F}}^{int}\} = \begin{Bmatrix} k_{t1}(\bar{w}_1 + r_1) + c_{t1}(\dot{\bar{w}}_1 + \dot{r}_1) \\ \vdots \\ k_{tnt}(\bar{w}_{nt} + r_{nt}) + c_{tnt}(\dot{\bar{w}}_{nt} + \dot{r}_{nt}) \\ 0 \\ \vdots \\ 0 \end{Bmatrix}_{ndv}, \tag{16}$$

where ndv is the number of degrees of freedom per vehicle. In equation (15), we assume that the ith wheel is always in contact with the bridge check. Replacing equations (11) and (12) into equation (16), we obtain

$$\{\bar{\mathbf{F}}^{int}\} = \begin{Bmatrix} k_{t1}(\langle \tilde{N}\rangle_1 [\boldsymbol{\Phi}]\{\mathbf{y}\} + r_1) + c_{t1}((v\langle \tilde{N}_{,x}\rangle_1 [\boldsymbol{\Phi}]\{y\} + \langle \tilde{N}\rangle_1 [\boldsymbol{\Phi}]\{\dot{\mathbf{y}}\}) + \dot{r}_1) \\ \vdots \\ k_{tnt}(\langle \tilde{N}\rangle_{nt} [\boldsymbol{\Phi}]\{\mathbf{y}\} + r_{nt}) + c_{tnt}((v\langle \tilde{N}_{,x}\rangle_{nt} [\boldsymbol{\Phi}]\{y\} + \langle \tilde{N}\rangle_{nt} [\boldsymbol{\Phi}]\{\dot{\mathbf{y}}\}) + \dot{r}_{nt}) \\ 0 \\ \vdots \\ 0 \end{Bmatrix}_{ndv}, \tag{17}$$

We define the vector

$$\{Z\} = \begin{Bmatrix} Z_l \\ Z_u \end{Bmatrix}, \tag{18}$$

where Z_l is the displacement vector corresponding to the degrees of freedom attached to the suspension and Z_u is the displacement vector corresponding to the degrees of freedom

attached to the rigid part of the vehicle, without the suspension. Equation (4) can be rewritten as

$$\begin{bmatrix} [\mathbf{M}_{vl}] & [\mathbf{M}_{vlu}] \\ [\mathbf{M}_{vul}] & [M_{vu}] \end{bmatrix} \begin{Bmatrix} \ddot{Z}_l \\ \ddot{Z}_u \end{Bmatrix} + \begin{bmatrix} [\mathbf{C}_{vl}] & [\mathbf{C}_{vlu}] \\ [\mathbf{C}_{vul}] & [\mathbf{C}_{vu}] \end{bmatrix} \begin{Bmatrix} \dot{Z}_l \\ \dot{Z}_u \end{Bmatrix} + \begin{bmatrix} [\mathbf{K}_{vl}] & [\mathbf{K}_{vlu}] \\ [\mathbf{K}_{vul}] & [\mathbf{K}_{vu}] \end{bmatrix} \begin{Bmatrix} Z_l \\ Z_u \end{Bmatrix} = \{\mathbf{F}_g\} + \{\overline{\mathbf{F}}^{tmt}\}. \tag{19}$$

The coupling of equations (14) and (19) gives a super-system containing the modal components of the bridge and the physical components of the vehicle. Using equations (14), (16) and (19), we obtain

$$\begin{bmatrix} [\mathbf{I}] & [\mathbf{0}] & [\mathbf{0}] \\ [\mathbf{0}] & [\mathbf{M}_{vl}] & [\mathbf{M}_{vlu}] \\ [\mathbf{0}] & [\mathbf{M}_{vul}] & [\mathbf{M}_{vu}] \end{bmatrix} \begin{Bmatrix} \ddot{y} \\ \ddot{Z}_l \\ \ddot{Z}_u \end{Bmatrix} + \begin{bmatrix} [\tilde{\boldsymbol{\chi}}]_{r\times r} & [\mathbf{A}_1]_{nt\times r} & [\mathbf{0}]^{-}_{nt\times r} \\ [\mathbf{A}_2]_{r\times nt} & [\mathbf{C}_{vl}] & [\mathbf{C}_{vlu}] \\ [\mathbf{0}]^{\mathrm{T}}_{r\times \overline{nt}} & [\mathbf{C}_{vul}] & [\mathbf{C}_{vu}] \end{bmatrix} \begin{Bmatrix} \dot{y} \\ \dot{Z}_l \\ \dot{Z}_u \end{Bmatrix}$$

$$+ \begin{bmatrix} [\tilde{\boldsymbol{\Omega}}]_{r\times r} & [\mathbf{B}_1]_{nt\times r} & [\mathbf{0}]^{-}_{nt\times r} \\ [\mathbf{B}_2]_{r\times nt} & [\mathbf{K}_{vl}] & [\mathbf{K}_{vlu}] \\ [\mathbf{0}]^{\mathrm{T}}_{r\times nt} & [\mathbf{K}_{vul}] & [\mathbf{K}_{vu}] \end{bmatrix} \begin{Bmatrix} y \\ Z_l \\ Z_u \end{Bmatrix} = \{F(x,t)\}, \tag{20}$$

with $\overline{nt} = ndv - nt$.

The previous submatrices are given by

$$[\tilde{\boldsymbol{\chi}}]_{r\times r} = \begin{bmatrix} \ddots & & \\ & 2\xi_j\omega_j & \\ & & \ddots \end{bmatrix} + [\mathbf{D}]_{r\times r}, \tag{21}$$

$$[\tilde{\boldsymbol{\Omega}}]_{r\times r} = \begin{bmatrix} \ddots & & \\ & \omega_j^2 & \\ & & \ddots \end{bmatrix} + [\mathbf{S}]_{r\times r}, \tag{22}$$

where the matrices [**D**] and [**S**] are given by

$$[\mathbf{D}] = [\boldsymbol{\Phi}]^{\mathrm{T}} \left(\sum_{j=1}^{nt} c_{tj} \{\tilde{N}\}_j \langle \tilde{N} \rangle_j \right) [\boldsymbol{\Phi}],$$

$$[\mathbf{S}] = [\boldsymbol{\Phi}]^{\mathrm{T}} \left(\sum_{j=1}^{nt} c_{tj} v \{\tilde{N}\}_j \langle \tilde{N}_{,x} \rangle_j + k_{tj} \{\tilde{N}\}_j \langle \tilde{N} \rangle_j \right) [\boldsymbol{\Phi}]$$

and

$$[\mathbf{A}_1] = [\mathbf{A}_2]^{\mathrm{T}} = -\begin{bmatrix} \langle \phi_1 \rangle \{\tilde{N}\}_1 c_{t1} & \cdots & \langle \phi_1 \rangle \{\tilde{N}\}_{nt} c_{tmt} \\ \vdots & \vdots & \vdots \\ \langle \phi_r \rangle \{\tilde{N}\}_1 c_{t1} & \cdots & \langle \phi_r \rangle \{\tilde{N}\}_{nt} c_{tmt} \end{bmatrix}, \tag{23}$$

$$[\mathbf{B}_1] = -\begin{bmatrix} \langle \phi_1 \rangle \{\tilde{N}\}_1 k_{t1} & \cdots & \langle \phi_1 \rangle \{\tilde{N}\}_{nt} k_{tmt} \\ \vdots & \vdots & \vdots \\ \langle \phi_r \rangle \{\tilde{N}\}_1 k_{t1} & \cdots & \langle \phi_r \rangle \{\tilde{N}\}_{nt} k_{tmt} \end{bmatrix}, \tag{24}$$

$$[\mathbf{B}_2] = [\mathbf{B}_1]^{\mathrm{T}} - v\begin{bmatrix} \langle \tilde{N}_{,x} \rangle_1 \{\phi_1\} c_{t1} & \cdots & \langle \tilde{N}_{,x} \rangle_1 \{\phi_r\} c_{t1} \\ \vdots & \vdots & \vdots \\ \langle \tilde{N}_{,x} \rangle_{nt} \{\phi_1\} c_{tnt} & \cdots & \langle \tilde{N}_{,x} \rangle_{nt} \{\phi_r\} c_{tnt} \end{bmatrix}. \tag{25}$$

The load vector is given by

$$\{F(x,t)\} = \begin{Bmatrix} \{0\}_{r\times 1} \\ \{F_g\}_{ndv\times 1} \end{Bmatrix} + \begin{Bmatrix} -[\mathbf{\Phi}]^{\mathrm{T}} \left(\sum_{i=1}^{nt} \{\tilde{N}\}_i (k_{ti} r_i + v c_{ti} r_{i,x}) \right) \\ \begin{Bmatrix} k_{t1} r_1 + v c_{t1} r_{1,x} \\ \vdots \\ k_{tnt} r_{nt} + v c_{tnt} r_{nt,x} \\ 0 \end{Bmatrix}_{ndv\times 1} \end{Bmatrix}_{(r+ndv)\times 1}. \tag{26}$$

Using the equations

$$\begin{Bmatrix} y \\ Z_l \\ Z_u \end{Bmatrix} = \begin{Bmatrix} y \\ Z_v \end{Bmatrix}, \tag{27}$$

the modified mass matrix can be expressed as

$$[\tilde{\mathbf{M}}(t)] = \begin{bmatrix} [\mathbf{I}] & \mathbf{0} \\ \mathbf{0} & [\mathbf{M}_v] \end{bmatrix}, \tag{28}$$

where $[\mathbf{M}_v]$ is the mass matrix of the vehicle. In compact form, we take $\langle \delta \rangle = \langle y Z_v \rangle$; thus the equations of motion of the coupled systems are defined as

$$[\tilde{\mathbf{M}}(t)]\{\ddot{\boldsymbol{\delta}}\} + [\tilde{\mathbf{C}}(t)]\{\dot{\boldsymbol{\delta}}\} + [\tilde{\mathbf{K}}(t)]\{\boldsymbol{\delta}\} = \{\mathbf{F}(x,t)\}. \tag{29}$$

The inverse of the modified mass matrix is known explicitly at each time step by

$$[\tilde{\mathbf{M}}(t)]^{-1} = \begin{bmatrix} [\mathbf{I}] & [\mathbf{0}] \\ [\mathbf{0}] & [\mathbf{M}_v] \end{bmatrix}^{-1} = \begin{bmatrix} [\mathbf{I}]^{-1} & [\mathbf{0}] \\ [\mathbf{0}] & [\mathbf{M}_v]^{-1} \end{bmatrix} = \begin{bmatrix} [\mathbf{I}] & [\mathbf{0}] \\ [\mathbf{0}] & [\mathbf{M}_v]^{-1} \end{bmatrix}, \tag{30}$$

where $[\tilde{\mathbf{M}}(t)]^{-1}$ remains constant until the number of vehicles changes. When a new nth vehicle reaches the bridge deck, the inverse of the modified matrix is easily computed:

$$[\tilde{\mathbf{M}}(t)]^{-1} = \begin{bmatrix} [\mathbf{I}] & \mathbf{0} & & & & \\ \mathbf{0} & [\mathbf{M}_v]_1^{-1} & & & & \\ & & \ddots & \mathbf{0} & & \\ & & \mathbf{0} & [\mathbf{M}_v]_s^{-1} & & \\ & & & & \ddots & \mathbf{0} \\ & & & & \mathbf{0} & [\mathbf{M}_v]_n^{-1} \end{bmatrix}. \tag{31}$$

1. *Initial calculation*

1.1 Form the matrices $[\mathbf{M}_b]$, $[\mathbf{C}_b]$ and $[\mathbf{K}_b]$ of bridge
1.2 Evaluate the natural frequencies and corresponding vibration modes: $[\mathbf{\Phi}]$ and $[\mathbf{\Omega}]$
1.3 Generate the profile of the road $r(x)$: $s_r(\omega_s) = A_r(\omega_s/\omega_{s0})^{-2}$
1.4 Set initial conditions
1.5 Choice the time step Δt

•**2.** *For each time step*

•**3.** *For each vehicle*

3.1 Determine the longitudinal position of each axle of the vehicle on the bridge
3.2 *For each new vehicle s*
Compute: $[\mathbf{M}_{vs}]$, $[\mathbf{K}_{vs}]$ and $[\mathbf{C}_{vs}]$ and the initial conditions
3.3 Form the vector $\{N\}_i$; $i = 1$, number of wheels in contact with the bridge
3.4 Compute the matrices: $[\mathbf{A}_1]$, $[\mathbf{A}_2]$, $[\mathbf{B}_1]$ and $[\mathbf{B}_2]$ (equations (23), (24) and (25))
3.5 Assemble the load vector $\{\mathbf{F}(x,t)\}$ (equation (26))
3.6 Form the modified matrices:

$$[\tilde{\mathbf{M}}(t)],\ [\tilde{\mathbf{K}}(t)] \text{ and } [\tilde{\mathbf{C}}(t)]$$

•**4.** Calculate effective loads at time t

$$\{\tilde{\mathbf{R}}_t\} = \{\mathbf{F}(x,t)\} - [\tilde{\mathbf{C}}(t)]\,\{\dot{\boldsymbol{\delta}}_t\} - [\tilde{\mathbf{K}}(t)]\,\{\boldsymbol{\delta}_t\}$$

4.1 Solve for accelerations at time t:

$$[\tilde{\mathbf{M}}(t)]\,\{\ddot{\boldsymbol{\delta}}_t\} = \{\tilde{\mathbf{R}}_t\}$$

4.2 Evaluate $\delta_{-\Delta t}$ when $t = 0$:

$$\{\boldsymbol{\delta}_{-\Delta t}\} = \{\boldsymbol{\delta}_0\} - \Delta t\,\{\dot{\boldsymbol{\delta}}_0\} + \frac{\Delta t^2}{2}\{\ddot{\boldsymbol{\delta}}_0\}$$

4.3 Evaluate displacements and velocities at time $t + \Delta t$:

$$\{\boldsymbol{\delta}_{t+\Delta t}\} = -\{\boldsymbol{\delta}_{t-\Delta t}\} - 2\,\{\boldsymbol{\delta}_t\} + \Delta t^2\,\{\ddot{\boldsymbol{\delta}}_t\}$$

$$\{\dot{\boldsymbol{\delta}}_{t+\Delta t}\} = \frac{\{\boldsymbol{\delta}_{t+\Delta t}\} - \{\boldsymbol{\delta}_t\}}{\Delta t}$$

*$t = t + \Delta t$

Figure 6. The computational algorithm for the coupled approach.

$[\mathbf{M}_v]_n^{-1}$ is a small matrix and it is simply stored in the corresponding vehicle routine. $[\tilde{\mathbf{M}}(t)]$ is called a pseudo-static mass matrix. To solve the system (29), we use an alternative step-by-step solution using the central difference method. The simplified algorithm is given in Figure 6.

4. NUMERICAL EXAMPLES

4.1. EXAMPLE 1: A TWO-DIMENSIONAL CASE

To validate the proposed formulation and its implementation, a dynamic analysis has been performed for a simply supported beam subjected to a two-foot (two degrees of freedom) system moving [9] at a constant speed (Figure 7). In the present example, the

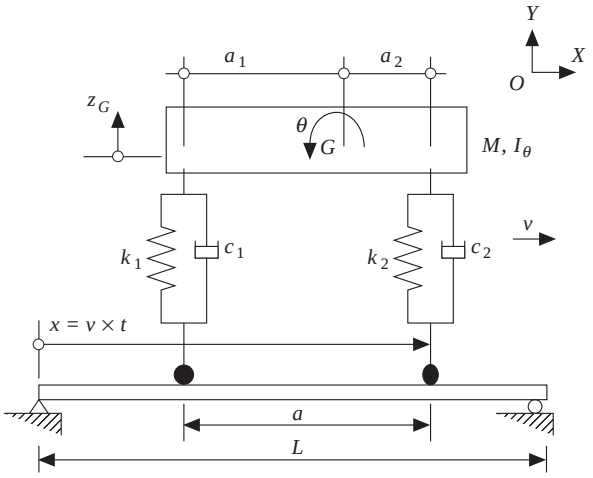

Figure 7. A beam subjected to a moving two-dof dynamic system.

velocity is represented by the speed parameter: $\alpha = T_1/\tau = vT_1/L$, where T_1 is the fundamental period of the beam and L is the length of the beam. The results from this analysis are compared with those shown in reference [9]. The parameters used for the simulation are shown in Table 1. To examine the effect of damping, two cases have been considered: case 1 without damping and case 2 with Rayleigh damping. Given the modal damping ratios for the first two modes, which may be determined by experimental modal analysis technique, the coefficients α and β can be computed [15].

The results obtained for case 1 are shown in Figures 8–10. Figure 8 shows the dynamic deflection at the centre of the beam for various speeds. The dynamic response of the moving system for the vertical displacements is shown in Figure 9. The response curves agree well with those found in reference [9]. The validity of the present formulation for a general moving dynamic system on a bridge can also be inferred from the rotational response of the moving system. As shown in Figure 8, the results agree well with those found in reference [9]. Those results provide further confidence that this new formulation and its implementation have been successful.

The impact factors obtained in the simulation (cases 1 and 2) are shown in Table 2 and Figure 11. As expected, those factors decrease with the presence of damping.

TABLE 1

Data for the problem with a beam subjected to a moving two-dof dynamic system

Data of the bridge	Data of the vehicle
$L = 1{\cdot}1938$ m	$g = 9{\cdot}81$ m/s^2
$\rho = 2{\cdot}9602 \times 10^3$ kg/m^3	$M = 5{\cdot}40247$ kg
$A = 0{\cdot}51 \times 10^{-2}$ m^2	$I_\theta = 0{\cdot}56825$ kg m^2
$I = 0{\cdot}9448 \times 10^{-8}$ m^4	$k_1 = 2{\cdot}164 \times 10^8$ N/m
$E = 10{\cdot}48 \times 10^{10}$ N/m^2	$k_2 = 1{\cdot}803 \times 10^8$ N/m
	$a_1 = 0{\cdot}348$ m, $a_2 = 0{\cdot}371$ m, $r(x) = 0$
Case 1	*Case* 1
$\xi_1 = \xi_2 = 0$	$c_1 = c_2 = 0$
Case 2	*Case* 2
$\xi_1 = 2\%$; $\xi_2 = 5\%$	$c_1 = 88{\cdot}68$ Ns/m, $c_2 = 78{\cdot}41$ Ns/m

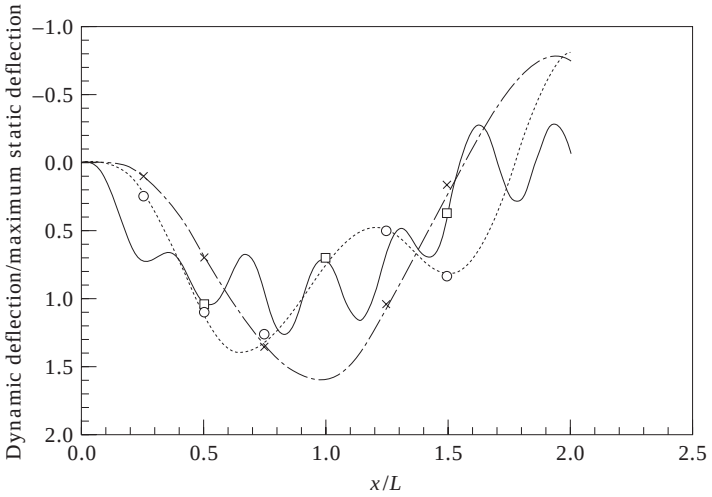

Figure 8. The central dynamic deflection of a simply supported beam subjected to a two-dof dynamic system, case 1: □, [9] $\alpha = 0{\cdot}31$; ○, [9] $\alpha = 1{\cdot}0$; ×, [9] $\alpha = 1{\cdot}5$; ——, $\alpha = 0{\cdot}31$; ---, $\alpha = 1{\cdot}0$; —·—, $\alpha = 1{\cdot}5$.

4.2. EXAMPLE 2: A THREE-DIMENSIONAL CASE

In this second example, we present the transient vibration of a bridge modelled with rectangular plate, discretized with 4×10 plate elements [16] (Table 3 and Figure 12). This structure is loaded by a moving three-dimensional vehicle system with seven degrees-of-freedom (Figure 2 and Table 4). In oder to validate the present formulation of the coupled method, the results are compared with those available in the literature using the uncoupled method [7, 8]. The vehicle crosses the bridge on the central line at a constant speed, and the first 20 natural frequencies have been selected in the analysis (Table 3).

First, we analyse the convergence of the central difference method. The stability condition [15] gives $\Delta t_{cr} = T_{20} \times 0{\cdot}318 = 0{\cdot}0034$ s. Results are shown in Figures 13–15 for the dynamic deflection at the plate centre point c for three different speeds of the vehicle.

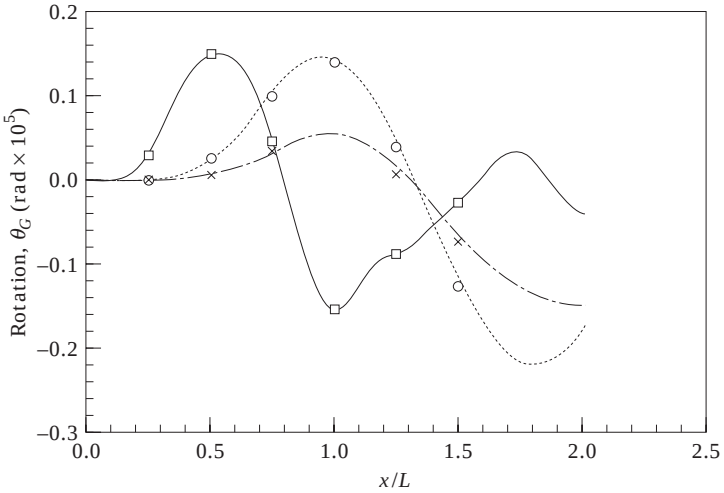

Figure 9. The rotational response of the two-dof moving dynamic system with a constant velocity, case 1: □, [9] $\alpha = 0{\cdot}31$; ○, [9] $\alpha = 1{\cdot}0$; ×, [9] $\alpha = 1{\cdot}5$; ——, $\alpha = 0{\cdot}31$; ---, $\alpha = 1{\cdot}0$; —·—, $\alpha = 1{\cdot}5$.

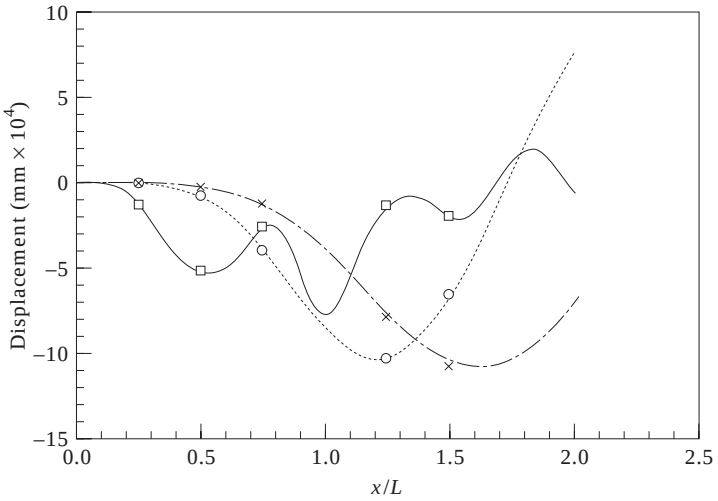

Figure 10. The vertical response of the two-dof moving dynamic system with a constant velocity, case 1: □, [9] $\alpha = 0{\cdot}31$; ○, [9] $\alpha = 1{\cdot}0$; ×, [9] $\alpha = 1{\cdot}5$; ——, $\alpha = 0{\cdot}31$; ---,, $\alpha = 1{\cdot}0$; —·—, $\alpha = 1{\cdot}5$.

TABLE 2

Impact factors for a simply supported beam crossed by a two-dof moving dynamic system

	Case 1		Case 2	
$\alpha = T_1/\tau$	Present method	Reference [9]	Present method	Reference [9]
0·31	1·266	1·246	1·214	1·173
1·0	1·396	1·381	1·361	1·342
1·5	1·603	1·582	1·560	1·535
2·0	1·685	1·665	1·635	1·616
2·5	1·667	1·651	1·619	1·601
3·0	1·610	1·590	1·570	1·550

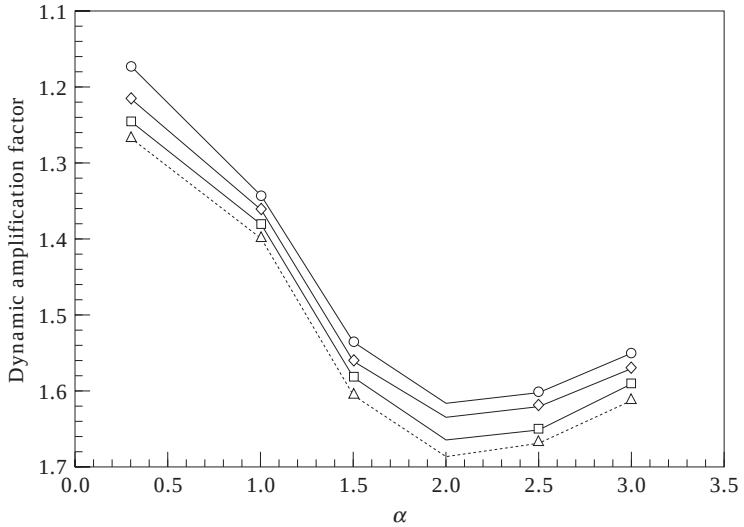

Figure 11. Dynamic amplification factors of a simply supported beam subjected to a two-dof moving dynamic system with a constant velocity ($\alpha = T_1/\tau$): △, case 1; ◇, case 2; □, [9] case 1; ○, [9] case 2.

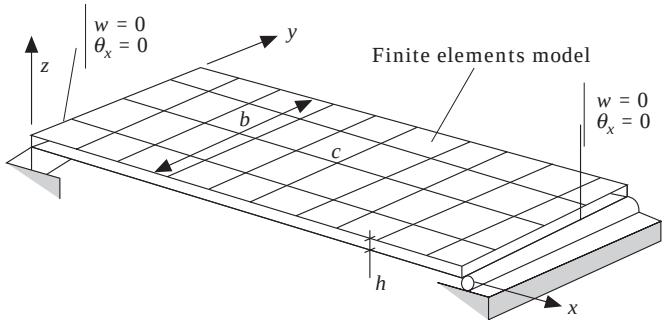

Figure 12. A plate bridge under a moving vehicle: $E = 3{\cdot}0 \times 10^{10}$ N/m^2, $\rho = 3500$ kg/m^3, $v = 0{\cdot}2$, $h = 0{\cdot}8$ m, $b = 8$ m and $L = 80$ m.

TABLE 3

Numerical results: *frequencies* (Hz)

Natural frequencies of the bridge	Natural frequencies of the vehicle
$f_1 = 0{\cdot}52$	$f_1 = 2{\cdot}310$ $f_5 = 5{\cdot}940$
$f_2 = 2{\cdot}16$	$f_2 = 2{\cdot}780$ $f_6 = 6{\cdot}810$
$\cdots$	$f_3 = 2{\cdot}978$ $f_7 = 7{\cdot}960$
$f_{20} = 93{\cdot}33$	$f_4 = 4{\cdot}954$

We should note that the response curves obtained by the coupled method (present formulation) are in good agreement with those obtained by the standard uncoupled method [6–8], using Newmark-β method and $\Delta t = 0{\cdot}01$ s. In Figure 13 a small difference is shown between results, using the uncoupled algorithm and coupled with a time step equal to 0.003 s, because vehicles move at low velocity; the behaviour of the bridge is a quasi-static case. At this velocity, the moving vehicle is equivalent to a concentrated propagation wave. However, this problem is easily resolved with Δt equal to 0·002 s.

Finally, in the second case, we analyse the influence of the high frequency of vehicle (f_{vmax}) on the stability conditions of the present formulation by changing the values of the stiffness coefficients of the vehicle. Two cases have been selected: $f_{vmax} = 79$ Hz and $f_{vmax} = 123$ Hz.

In the first case, the results for the dynamic deflection are shown in Figure 16. All the curves are the same when the time step used is less than or equal to Δt_{cr}.

TABLE 4

Data of vehicle with seven dof (*Figure* 2)

$g = 9{\cdot}81$ m/s^2, $Mv = 1460$ kg
$I_\theta = 1516$ Nms^2, $I_\alpha = 449$ kg m^2
$k_1 = k_2 = k_3 = k_4 = 0{\cdot}399 \times 10^6$ N/m
$k_{t1} = k_{t2} = k_{t3} = k_{t4} = 0{\cdot}351 \times 10^6$ N/m
$c_1 = c_3 = 23\,210$ Ns/m, $c_2 = c_4 = 5180$ Ns/m
$c_{t1} = c_{t2} = c_{t3} = c_{t4} = 800$ Ns/m
$m_1 = m_3 = 800$ kg, $m_2 = m_4 = 710$ kg
$a_1 = 0{\cdot}35$, $a_2 = 0{\cdot}65$ m, $a_3 = a_4 = 0{\cdot}5$
$s_1 = 2{\cdot}66\,m$, $s_2 = 1{\cdot}5\,m$, $h_v = 1{\cdot}2$ m

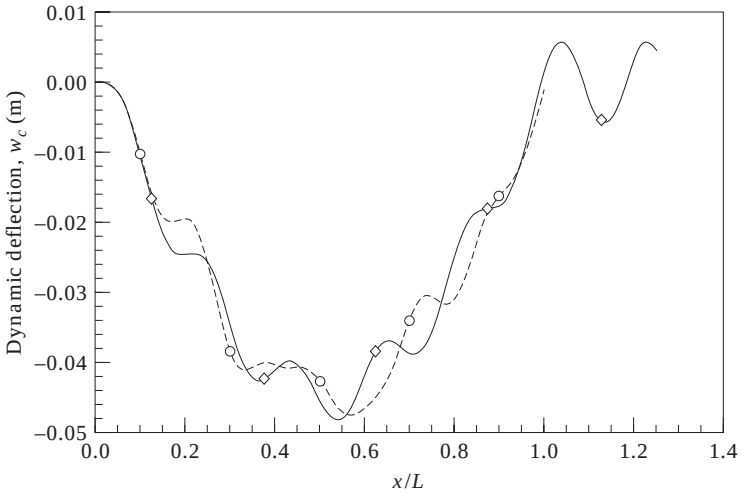

Figure 13. The vertical central deflection w_c of the bridge as a function of vehicle position; vehicle speed $v = 8$ m/s: ○, coupled method, $\Delta t = 0{\cdot}03$ s; ——, modal uncoupled method, $\Delta t = 0{\cdot}01$ s; ◇, coupled method, $\Delta t = 0{\cdot}02$ s.

The results of the second case are shown in Figure 17. We observe the numerical instability phenomena because the selected time step fails to integrate all modes. The calculated response is therefore expected to be unbounded because the highest frequency of the vehicle is greater than the highest frequency of the bridge. In fact, the time step does satisfy the stability criterion when $\Delta t \leqslant T_{max} \times 0{\cdot}318 = 0{\cdot}0034$ s, and $T_{max} = \text{Max}\,(T_{veh}, T_{Bridge})$. In this case we find that this value is controlled by the vehicle value: $\Delta t_{cr} = (1/123) \times 0{\cdot}318 = 0{\cdot}00258$ s. This problem is usually avoided because, in practice, the highest selected frequency of the bridge should be greater than those of the vehicles.

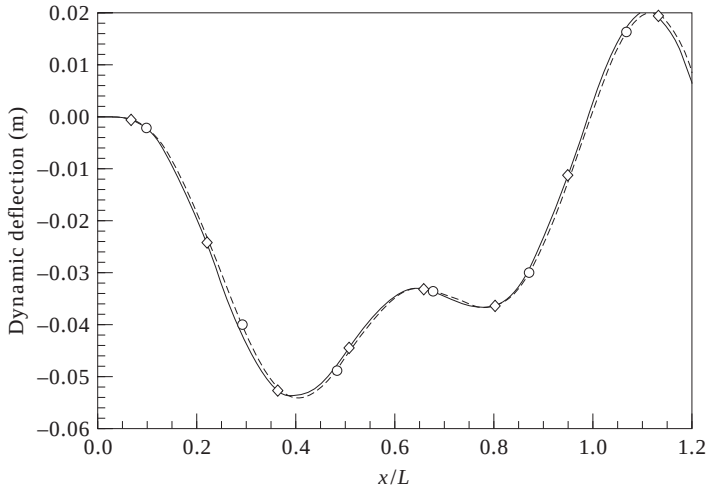

Figure 14. The vertical central deflection w_c of the bridge as a function of vehicle position; vehicle speed $v = 20$ m/s: ○, coupled method, $\Delta t = 0{\cdot}03$ s; ◇, uncoupled method, $\Delta t = 0{\cdot}01$ s.

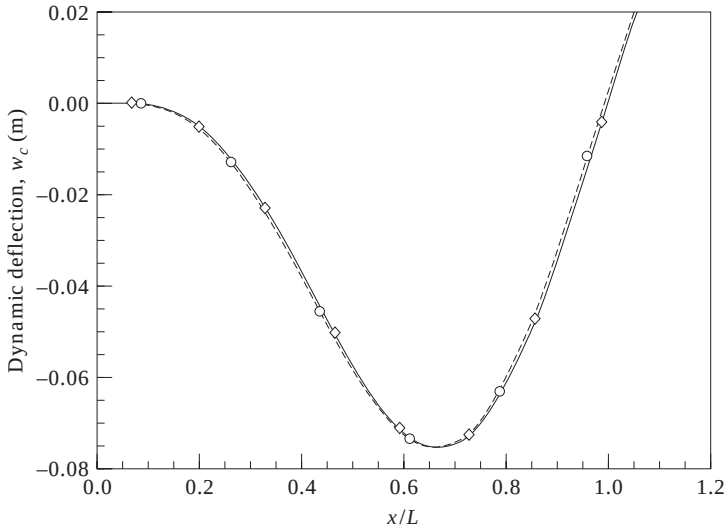

Figure 15. The vertical central deflection w_c of the bridge as a function of vehicle position; vehicle speed $v = 40$ m/s: ○, coupled method $\Delta t = 0{\cdot}03$ s; ◇, uncoupled method $\Delta t = 0{\cdot}01$ s.

4.3. REMARKS

In this paragraph we present computational results to compare the proposed method to the uncoupled iterative method.

Example 2 *of this paper*: an example of transient vibrations of a plate simply supported under the effect of 3-D moving vehicles with seven degrees of freedom (Figure 12).

Two-beam mixed bridge [7]: an example of transient vibration of a bridge with one-span simply supported beam under the effect of 3-D moving vehicles with seven degrees of freedom; the bridge is modelled with finite element shells [16] and 3-D beams elements [7, 18], (Figure 18).

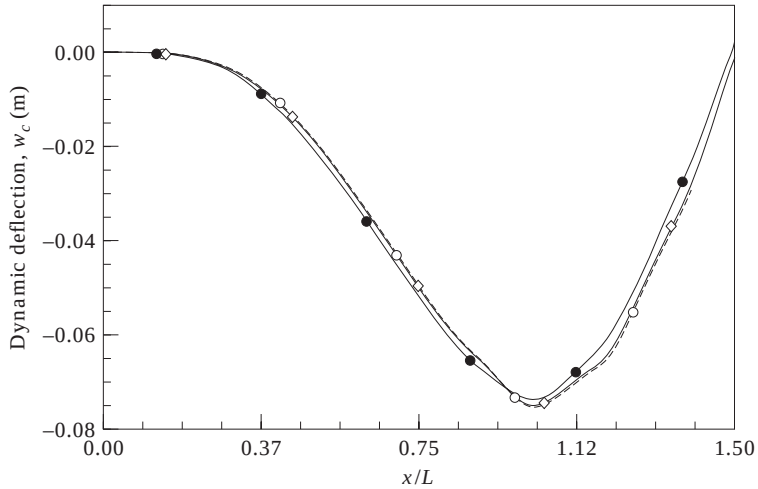

Figure 16. The vertical central deflection w_c of the bridge as a function of vehicle position (vehicle speed: $v = 80$ m/s) where $f_{vmax} = 79$ Hz: ○, coupled method, $\Delta t = 0{\cdot}0014$ s; ◇, coupled method, $\Delta t = 0{\cdot}0014$ s; ●, coupled method, $\Delta t = 0{\cdot}003$ s.

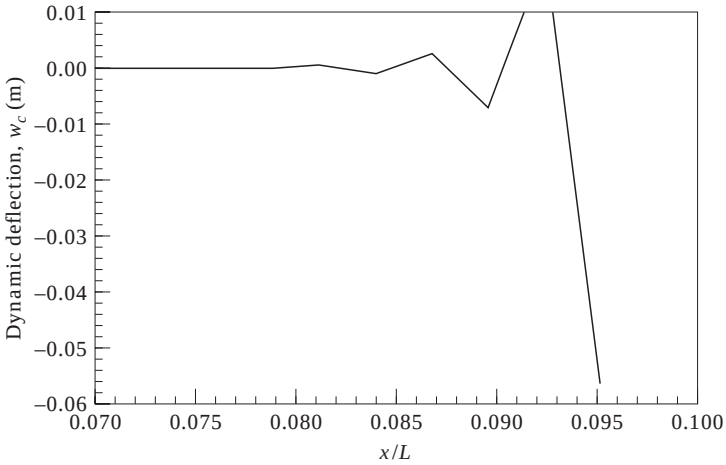

Figure 17. The instability of the central difference method in the coupled formulation problem ($v = 80$ m/s), where $f_{vmax} = 123$ Hz.

Senneterre concrete bridge, *Quebec*, *Canada* [7, 18]: an example of transient vibration of a bridge with three independent spans simply supported under the effect of 3-D moving vehicles with seven degrees of freedom; the bridge is modelled with finite element shells [16] and 3-D beam elements [7, 18] (Figure 19).

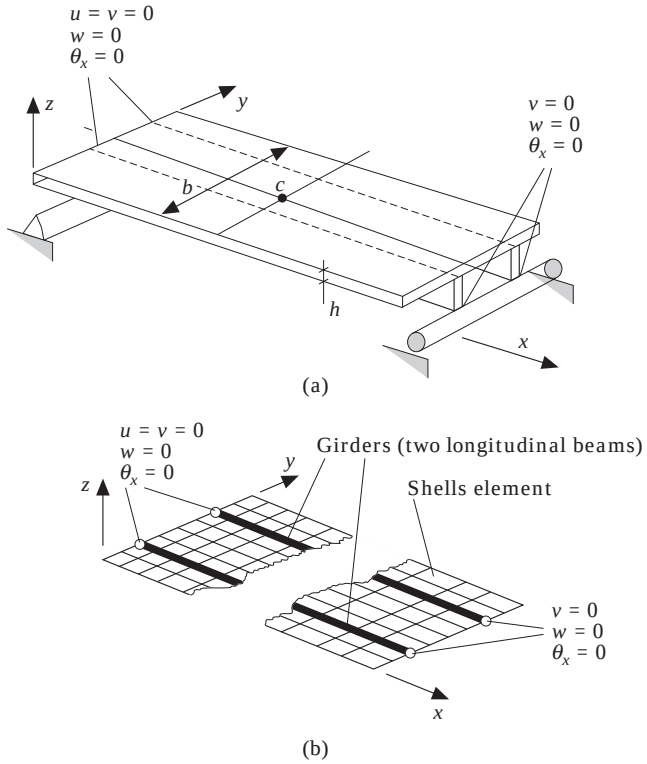

Figure 18. A two-beam mixed bridge under a moving vehicle: (a) bridge; (b) model.

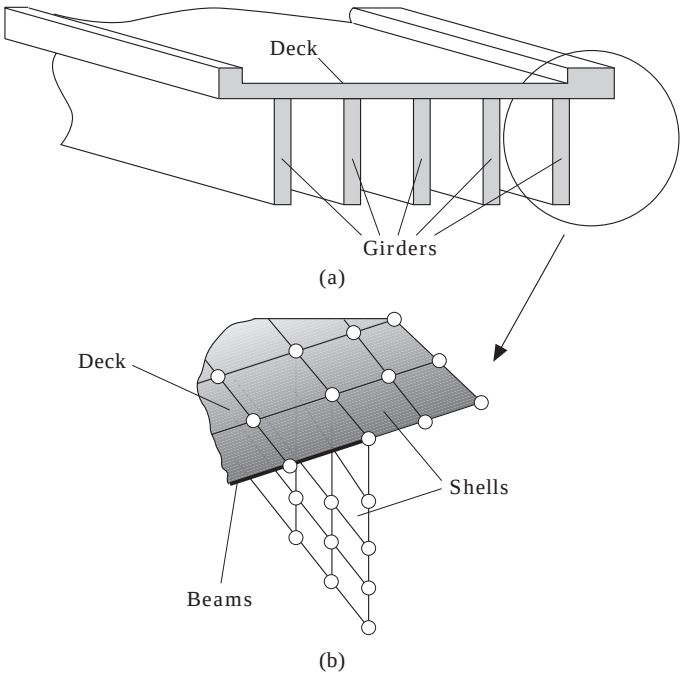

Figure 19. The Senneterre concrete bridge: (a) bridge model and transverse section representation; (b) finite element representation.

We conclude from table 5 that: in all cases the uncoupled iteration method applied in the full space (no modal reduction) takes the highest computational time; except for the first case, the fully coupled method (without any iteration) is the most performant one; and the modal uncoupled iteration method is more efficient than the full space uncoupled iteration method.

TABLE 5

Relative computational times for transient vibrations of different bridges, using coupled and uncoupled methods

	Relative CPU time	Characteristics
(a) Plate example		
Coupled method	0·5	20 modes
Modal uncoupled iterative method	0·5	20 modes
Uncoupled iterative method	1·0	145 degrees of freedom
(b) Two-beam mixed bridge		
Coupled method	0·3	10 modes
Modal uncoupled iterative method	0·4	10 modes
Uncoupled iterative method	1·0	1134 degrees of freedom
(c) Senneterre concrete bridge		
Coupled method	0·2	8 modes
Modal uncoupled iterative method	0·3	8 modes
Uncoupled iterative method	1·0	5166 degrees of freedom

5. CONCLUSIONS

A general finite element formulation for the solution of the dynamic interaction problem between a bridge and vehicles has been presented. It is based on a new and original coupled component approach using a modified pseudo-static mass matrix. A central difference scheme is used successfully to solve this problem.

Numerical simulation results obtained from the proposed formulation are in excellent agreement with those reported in the literature. This validates the procedure and its implementation presented in the paper. The formulation is general because it is available for all kinds of dynamic systems of vehicles, and also because it duly considers the bridge pavement as a random surface irregularity.

This new formulation with the suggested organization of the components, introduces the use of the central difference method very appropriately, since the inverse of the pseudo-static mass matrix is known at each time step without any numerical endeavour.

There is no limitation concerning the complexity (number of dof) of the bridge structure to be analyzed if the stability criterion can be estimated and satisfied.

REFERENCES

1. J. S. Fenves, A. S. Veletsos and S. P. Siess 1962 *Dynamic Studies of Bridge on the AASHO Road Test*, *Highway Research Board*, Reports **71** and **73**, Washington, D.C.: National Academy of Sciences.
2. F. G. A. Fleming and J. P. Romualdi 1961 *American Society of Civil Engineering*. *Journal of Structural Division* **87**(7), 31–60. Dynamic response of highway bridges.
3. A. S. Veletsos and T. Huang 1970 *American Society of Civil Engineering*. *Journal of Eng. Mech. Div.*, *ASCE*. **90**(5), 1648–1659. Analysis of dynamic response of highway bridges.
4. P. Paultre, J. Proulx and M. Talbot 1995 *American Society of Civil Engineering*, *ASCE Journal of Structural Engineering* **121**(2), 362–376. Dynamic testing procedures for highway bridges using traffic loads.
5. M. Fafard, Mallikarjuna and M. Savard 1993 *Proceedings of the EURODYN'93 Structural Dynamics*. *Trandheim Balkema*, *Rotterdam*, *The Netherlands* **2**, 951–960. Dynamic of bridge–vehicle interaction.
6. T. Boudjelal, M. Fafard and A. Gakwaya 1996 *Proceedings of the EURODYN'96. Structural Dynamics*, *Florence*, *Italy*, 767–774. Modelling of damping and its applications to dynamic bridge–vehicle interaction.
7. K. Henchi 1995 *Ph.D. Thesis*, *Department of Applied Mechanics*, *Compiegne University of Technology*, *France*. Dynamics analysis of bridges under moving vehicles by a finite elements method.
8. K. Henchi, M. Fafard and M. Talbot 1998 *Canadian Journal of Civil Engineering* (*in press*). Dynamic analysis of the bridge–vehicles interaction for the highway bridges, Part I: numerical aspects (in French).
9. Y. H. Lin and M. W. Trethewey 1990 *Journal of Sound and Vibration* **136**, 323–342. Finite element analysis of elastic beams subjected to moving dynamic loads.
10. M. Fafard, M. Bennur and M. Savard 1997 *International Journal of Engineering Computations* **14**(5), 491–508. A general multi-axle vehicle model to study the bridge–vehicle interaction.
11. E. Akoussah, M. Fafard, M. Talbot and D. Beaulieu 1997 *Canadian Journal of Civil Engineering* **24**(2), 313–322. Parametric study of the dynamic amplification factor of single span concrete bridges (in French).
12. T. L. Wang, D. Huang and M. Shahawy 1992 *American Society of Civil Engineering*. *Journal of Structural Engineering*. **118**(8), 2222–2238. Dynamic response of multigirder bridges.
13. C. J. Dodds and J. D. Robson 1973 *Journal of Sound and Vibration* **31**, 175–183. The description of road surface roughness.
14. H. Honda, Y. Kajikawa and T. Kobori 1982 *American Society of Civil Engineering*, *Journal of Structural Engineering* **108**(9), 1956–1966. Spectra of road surface roughness on bridges.
15. R. W. Clough and J. Penzien 1993 *Dynamics of Structures*. New York: McGraw-Hill.

16. M. TALBOT, G. DHATT and K. HENCHI 1992 *Annual Conference of the Canadian Society for Civil Engineering*, *May* 27–29, *Québec*, *QC*. A new shell element applied to the 3-D analysis of bridges–structures.
17. K. HENCHI, W. HOORPAH, G. DHATT and M. TALBOT 1996 *Proceedings of the* 4*th National Congress of AFPS*, *Seismic*, *Engineering and Vibrations Aspect in Civil Engineering*, *Saint-Rémy-lès Chevreuse*, *France*, 10–12 April, 283–292. Computational dynamics of structures under moving loads by the finite element method (in French).
18. K. HENCHI, M. FAFARD and M. TALBOT 1998 *Canadian Journal of Civil Engineering* (in press). Dynamic analysis of the bridge–vehicles interaction for the highway bridges, part II: application to the Senneterre bridge in Quebec (in French).

APPENDIX: NOTATION

dof	degrees of freedom
$S_r(\omega_r)$	power spectral density of the road surface (m^2/cycle/m)
A_r	roughness coefficient (m^2/cycle/m)
ω_s	spatial frequency (cycle/m)
ω_{so}	discontinuity frequency (= 1/2)
FFT	Fast Fourier Transform
$r(x)$	road profile (m)
$\Delta\omega_s$	frequency step
$[\mathbf{M}_v]$, $[\mathbf{C}_v]$, $[\mathbf{K}_v]$	mass, damping and stiffness matrices of the vehicle
$\{\mathbf{Z}\}$, $\{\dot{\mathbf{Z}}\}$, $\{\ddot{\mathbf{Z}}\}$	vertical displacement, velocity and acceleration vectors of the vehicle
$\{\mathbf{F}_g\}$	force vector caused by the effect of the gravitation
$\{\bar{\mathbf{F}}^{int}\}$	interaction force vector applied on the vehicle
$[\mathbf{M}_b]$, $[\mathbf{C}_b]$, $[\mathbf{K}_b]$	mass, damping and stiffness matrices of the bridge
$\{\mathbf{u}\}$, $\{\dot{\mathbf{u}}\}$, $\{\ddot{\mathbf{u}}\}$	vertical displacement, velocity and acceleration vectors of the bridge
$[\mathbf{\Phi}]$	matrix of the r eigenvectors of the structure
$[\mathbf{\Phi}^e]$	matrix of the r eigenvectors of the element e
$\{y\}$	modal response
$\langle\tilde{\mathbf{N}}\rangle_i$, $\langle\mathbf{N}\rangle_i$	shape fractions evaluated at the contact point i (dimensions of $\langle\tilde{\mathbf{N}}\rangle_i$) and $\langle\mathbf{N}\rangle_i$ are respectively the total number of dof and the total number of nodes per element
k_{ti}, c_{ti}	tire stiffness and damping coefficient of the ith wheel
$\bar{w}_i$	vertical displacement at the ith wheel
r_i	road surface roughness under the ith wheel
$\{\bar{\mathbf{F}}_{bv}^{int}\}$	interaction force applied on the bridge by the ith wheel
ndv	number of degrees of freedom per vehicle
nt	number of wheels or tires per vehicle
ω_j	jth pulsation of the bridge
$[\mathbf{D}]$	numerical damping matrix
$[\tilde{\mathbf{M}}]$	modified mass matrix
Δt	time step
T_{max}	maximum period